Journal of Cerebral Blood Flow & Metabolism (2015) 35, 1862–1870

www.jcbfm.com

OPEN

ORIGINAL ARTICLE

Metabolic changes in early poststatus epilepticus measured by MR spectroscopy in rats

Yijen Wu[1], Patrice S Pearce[2], Amedeo Rapuano[3], T Kevin Hitchens[4], Nihal C de Lanerolle[3] and Jullie W Pan[2]

There is little experimental *in vivo* data on how differences in seizure duration in experimental status epilepticus influence metabolic injury. This is of interest given that in humans, status duration is a factor that influences the probability of subsequent development of epilepsy. This question is studied using 7-T magnetic resonance (MR) spectroscopy, T2 relaxometry in the incremented kainate rodent model of temporal lobe epilepsy, using two durations of status epilepticus, 1.5 and 3 hours. Histologic evaluation was performed in a subset of animals. Three days after status, single-voxel (8 mm^3) point resolved spectroscopy (PRESS) MR spectroscopic measurements were acquired at 7 T to assess the cerebral metabolites measured as a ratio to total creatine (tCr). The status injury resulted in decreased *N*-acetylaspartate NAA/tCr, increased myo-inositol/tCr and glutamine/tCr, increased T2, and significant declines in NeuN-stained neuronal counts in both status groups. Regressions were identified in the status groups that provide evidence for neuronal injury and astrocytic reaction after status in both the short and long status duration groups. The long status group displays changes in glutathione/tCr that are not identified in the short status group, this difference possibly representing a maturation of injury and antioxidant response that occurs in synchrony with glutamatergic injury and glial activation.

Journal of Cerebral Blood Flow & Metabolism (2015) **35,** 1862–1870; doi:10.1038/jcbfm.2015.145; published online 24 June 2015

Keywords: energy metabolism; epilepsy; glutamate; magnetic resonance spectroscopy; neuronal–glial interactions

INTRODUCTION

Among the many pathophysiologic abnormalities found in epilepsy and the region of seizure onset, metabolic dysfunction is common. Although it is known that seizures themselves impose significant demand on bioenergetics and can cause such metabolic injury, whether and how this dysfunctional metabolism has a role in epileptogenesis remains an area of work. Metabolic and mitochondrial dysfunction has many consequences that can result in hyperexcitability,[1–3] including decreased neuronal ATP that fails to maintain ionic homeostasis and membrane potential, reactive oxygen species that injure membrane lipids and proteins resulting in aberrant excitability, aberrant function of glutamine (Gln) synthetase that can potentially distort levels of glutamate (Glu), Gln, or neurotransmitter cycling, or aberrant calcium handling that results in abnormal synaptic activity. As shown by several groups,[4,5] it has been suggested that ^{1}H magnetic resonance (MR) spectroscopy and imaging (MRI) may be informative for studying these processes.

In this report, we assessed the variability of metabolic injury in experimental status epilepticus (SE) in the poststatus early epileptogenesis time period using magnetic resonance studies. The nature of this variability is of interest, as understanding the effect of a variable initial insult can give some insight on the SE injury process and the initiation of epileptogenesis. This is also of pertinence given the epidemiologic studies of human febrile seizures, finding that complexity of seizure (generalized versus focal onset), duration, or multiple events, which (while not clear enough for clinical prognostication in human patient groups) influences the probability of subsequent development of epilepsy.[6] To this end, we used the multiple low-dose intraperitoneal kainate model of temporal lobe epilepsy.[7] This SE protocol has been studied with continuous EEG monitoring[8] finding the presence of nonconvulsive seizures within 9 days (8.3 ± 0.9 days) after status, and onset of motor seizures at a more variable 18.3 ± 10.2 days. We thus used this model because of these well-defined features in addition to its known hippocampal degeneration, gliosis, axonal sprouting, and comparatively low mortality.

With the intraperitoneal dosing protocol, the kainate chemoconvulsant model exhibits variability, which is believed to be due in part to bioavailability of the kainate.[9] For example, Kondratyev and Gale[10] found that the nature of DNA fragmentation depended on the latency to status onset. As a result of this variability, it should be noted that the observed data are effectively cross-sectional in nature, i.e., there is an anticipated spread in the group measurements resulting from interanimal differences in temporal onset of seizures. Analysis of such cross-sectional data commonly uses group and correlation testing to identify and classify how measured parameters, e.g., neuronal versus glial metabolic parameters synchronously respond to the SE insult. Thus, in the present data, we anticipate measuring a correlated spread of metabolic parameters that are most likely components of neuronal and astrocytic processes. To further widen the variability in this model with a view toward understanding how lesser versus greater seizure injury affects metabolism in the poststatus period (and ultimately epileptogenesis), we tested this model using 1.5- and 3-hour periods of SE. Three days later, we acquired short and moderate echo (TE 10 ms, 40 ms, respectively) single-voxel ^{1}H MR spectroscopy of the CA3 and CA1 region of the dorsal

[1]Department of Developmental Biology, University of Pittsburgh School of Medicine, Pittsburgh, Pennsylvania, USA; [2]Departments of Neurology and Radiology, University of Pittsburgh, Pittsburgh, Pennsylvania, USA; [3]Department of Neurosurgery, Yale University School of Medicine, New Haven, Connecticut, USA and [4]Pittsburgh NMR Center for Biomedical Research, Carnegie Mellon University, Pittsburgh, Pennsylvania, USA. Correspondence: Dr JW Pan, Departments of Neurology and Radiology, University of Pittsburgh, Suite 811 Kauffman Building, 3471 Fifth Avenue, Pittsburgh, Pennsylvania 15213, USA.
E-mail: Jwp44@pitt.edu
This work was supported by National Institutes of Health R21 NS083035, R01 NS090417 (JWP), and P41 EB001977 (KH).
Received 11 February 2015; revised 17 May 2015; accepted 20 May 2015; published online 24 June 2015

hippocampus. In subsets of these animals, we also performed quantitative T2 relaxometry over the hippocampal slice and evaluated the extent of histologic injury with NeuN (Neuronal nuclei) and Fluoro-Jade B (both stains, Millipore, Temecula, CA, USA) staining in the hilus.

For the interpretation of spectroscopic data, the detected metabolites have reasonably well-understood functions. *N*-Acetylaspartate and *N*-acetyl aspartyl glutamate (NAA+NAAG, dominated by the NAA component), is a measure of neuronal mitochondrial function, with decrements found in many human and animal studies of various neurologic disorders and epilepsy.[11–13] Glutamate as the primary excitatory neurotransmitter in glutamatergic neurons and a key energy-generating metabolite, traverses both the neuronal and astrocytic compartments. With concentrations of Glu of ~9 mM/L in gray matter,[14] Glu identifies the large glutamatergic neuronal pool; similarly gamma aminobutyric acid (GABA) identifies the GABAergic neuronal pool. Total creatine (sum of phosphocreatine and creatine) comprises the requisite components of the creatine kinase reaction (the enzymatic system to buffer changes in ATP concentrations) is also found in both neuronal and astrocytic compartments. As discussed by Connett,[15] normalization to total creatine provides relevant assessments of many bioenergetic compounds, which is also pertinent for many compounds that interact with ATP and therefore are supported by the creatine kinase system. In this context, the normalization is taken relative to the size of the tissue's creatine

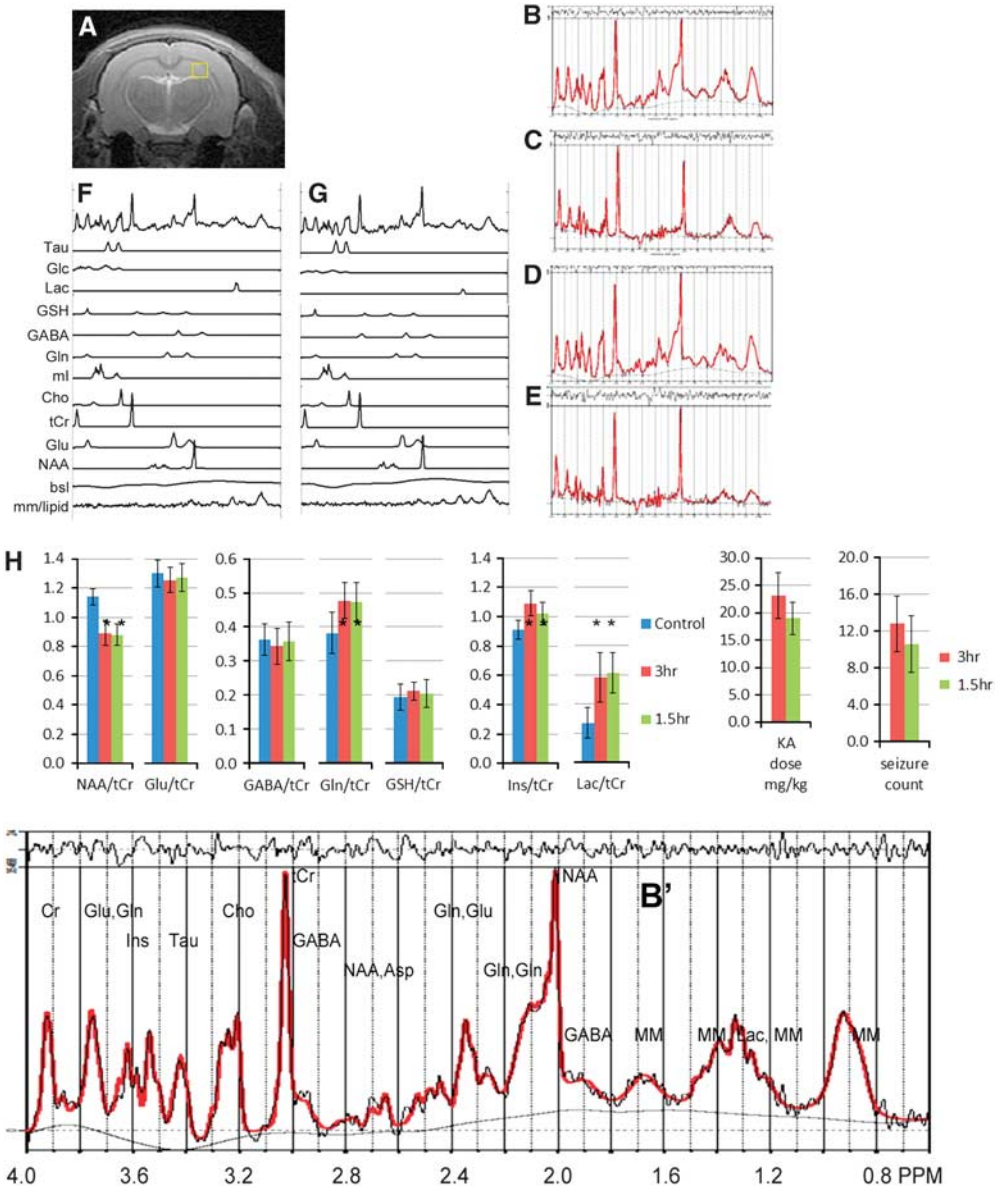

Figure 1. (**A**) Scout: the box indicates the approximate position and size of the 2 × 1.8 × 2.2 mm voxel. (**B** and **C**) TE 10 ms and TE 40 ms spectra from a kainate 3-hour rat; (**D** and **E**) TE 10 ms and TE 40 ms spectra from a control rat. Each of the spectra from **B** to **E** show the experimental (black), fitted (red), baseline (bottom), and residual (top of each of spectrum). Note: the spectrum in **B** is shown in greater detail on the bottom as **B**′ with identification of key metabolites. (**F** and **G**) show the LCM results of a TE 10 ms spectrum from a 3-hour and control animal, respectively showing individual metabolite fits, baseline, and macromolecule/lipid components. (**H**) Column plots of the group means, kainate dosing, and seizure counts (stage 3/4/5 (ref. 21)). *$P < 0.001$ in comparison to control: shown are NAA/tCr, Glu/tCr, GABA/tCr, Gln/tCr, GSH/tCr, Ins/tCr, and Lac/tCr. Also shown are the column plots for kainate dosing and number of seizures. GABA, gamma-aminobutyric acid; Gln, glutamine; Glu, glutamate; GSH, glutathione; Ins, myo-inositol; KA, kainate acid; NAA, *N*-acetylaspartate with *N*-acetylaspartate glutamate; tCr total creatine (phosphocreatine and creatine).

kinase buffering system. As a result, the measurements are best considered not as absolute concentrations but rather as an index of its function, which needs to be compared with control. Glutamine and myo-inositol (Ins) are identified as predominantly astrocytic compounds functioning to support neurotransmitter Glu clearance and responding to osmotic conditions.[16,17] Other compounds of interest (glutathione (GSH) and lactate) are also well known and will be discussed below in context.

As is commonly used in clinical MRI, T2-weighted contrast is used in brain imaging to assess for edema, neuronal injury, and gliosis seen in traumatic brain injury, ischemia, and seizures. The T2 or transverse relaxation time is a biophysical parameter that characterizes the time constant by which the transverse MR signal decays. The value of the water T2 is a consequence of molecular tumbling and is influenced by many factors in living tissue, such as osmolality and interactions with the surrounding environment.[18,19] T2-weighted brain MR images are bright in cerebrospinal fluid-filled spaces, gray matter to a larger extent than white matter, bright in areas of edema, and in many types of pathologic assessment since many of these tissue states have highly mobile water molecules and exhibit long T2 values. In both clinical and experimental epilepsy, T2-weighted imaging and relaxometry have been shown related to seizure injury and possibly to epileptogenesis.[4,20] In this study, we used T2 relaxometry to correlate with metabolic profiles as well as histopathologic changes after kainate-induced seizure.

MATERIALS AND METHODS

Model

Male 6- to 7-week-old, 180-200g Sprague Dawley rats (Charles River, Wilmington, MA, USA) were used throughout. Animals were housed in standard rectangular single cages throughout with 12-hour light/dark cycle. After a 2-day post-arrival acclimation period, animals were handled daily until model preparation. At this point, rats weighed on average 190 ± 20 g. As per the incremented kainate model (8), animals were injected hourly with 5 mg/kg kainate (prepared in sterile saline) until a stage (Racine[21]) 3/4/5 seizure was elicited. The timing of SE started after this first stage 3/4/5 seizure and ended 1.5 or 3 hours after this first seizure. The number of seizures in the previous hour determined the dose kainate received in the following hour: if the rat had 0 to 5 seizures, a full dose of 5 mg/kg was administered; if it had >5 seizures, a half dose of 2.5 mg/kg was administered. If the rat was observed to be rapidly jumping in place (popcorning) or circling the cage, the dose for that hour was skipped as these behaviors usually precede death. For a 3-hour status rat, the typical duration of the entire process was 7 to 8 hours, requiring 2 to 3 hours before the start of the status period. Figure 1H shows the total doses of kainate for each group. Control rats were equivalently treated with sterile saline. Seizures were terminated with subcutaneous 10 mg/kg diazepam, which eliminated all behavioral seizures for both the 1.5- and 3 hour animals and resulted in apparent sedation. Rats were then given 5mL warmed subcutaneous lactated Ringer's solution (Henry Schein, Melville, NY, USA), and returned to their home cage. After SE, rats were weighed daily and given 5 mL warmed lactated Ringer's solution, and moistened rat chow to facilitate recovery. Up to the completion of imaging, we experienced a mortality rate of 7%, which is below the anticipated 15% projected for this model.[7] ARRIVE (Animal Research: Reporting of In Vivo Experiments) guidelines were used throughout this project.

Three days after SE, animals underwent the imaging study, with all studies performed between 0800 to 1500 hours, with the delay needed for transfer between the home cage and imaging facility being <3 minutes. Rats were briefly anesthetized with isoflurane, intubated, and secured in a cradle for MRI. Anesthesia was maintained by adjusting isoflurane to 2%, N_2O at 50 mL/min and O_2 at 200 mL/min. A rectal thermal probe was used to monitor temperature, which was linked with feedback control to a warmed air source to maintain a body temperature of 37°C. After imaging rats were perfused transcardially with 4% buffered paraformaldehyde, pH 7.4, and the brains were harvested for histologic staining with cryoprotectant storage at -20°C.

A subset of animals ($n=4$, 1.5 hours; $n=5$, 3 hours) were evaluated with NeuN and Fluoro-Jade B histologic analysis. At 300-μm intervals, 50-μm thick slices through the hippocampus were stained with Fluoro-Jade B for the localization of degenerating neurons.[22] A similar adjacent series was immunostained with an antibody to NeuN (1:1,000) with the biotinylated avidin–biotin technique (Vector Labs, Burlingame, CA, USA) and the glucose oxidase–DAB–Nickel methods for visualization.[23] A subset of animals was also immunostained to glial fibrillary acidic protein to assess for glial injury and activation. For consistency in this initial evaluation, neuronal counts were taken in the hilar region using a stereological technique (Stereo Investigator, MBF Bioscience, Williston, VT, USA) and expressed as the number of stained neurons per mm^2.

All animal experiments were approved by the Institutional Animal Care and Use Committee at the University of Pittsburgh (PHS Assurance A3187-01) and Carnegie Mellon University, and were conducted in accordance with the US Public Health Service's Policy on Humane Care and Use of Laboratory Animals. No adverse events were noted during this study.

Spectroscopy

A Bruker Biospec 7-T 40-cm horizontal MR system (Billerica, MA, USA) was used throughout with a 72-mm volume transmit coil and two-element receiver array. After initial three-direction (Tripilot) localizer acquisitions, T2-weighted RARE (rapid acquisition with relaxation enhancement multiple spin echo) acquisitions were acquired for optimal placement to position the slice of interest in the hippocampus as shown in Figure 1A. Static field homogeneity shimming was performed using Bolero,[24] a noniterative field map calculation that optimized first- and second-degree shim values. As performed over the hippocampal slice (Figure 1), the typical s.d. of the B0 field was 6.2 ± 1.7 Hz (10 animals). With the available transmit strength of 1500 Hz, single-voxel PRESS spectroscopic 8 mm^3 (typically, $2 \times 2 \times 2$ or $2 \times 1.8 \times 2.2$ mm) acquisitions (17 minutes per acquisition) at TE 10 ms and 40 ms were performed separately over the left and right hippocampus. Water suppression was performed using a VAPOR prespin echo sequence. LCM (http://s-provencher.com/pages/lcmodel.shtml)[25] analysis was performed for determination of the metabolite profiles and taken as a ratio to total creatine. Analyses were performed without identification as to animal grouping and metabolites with a Cramer–Rao bound $>10\%$ were omitted from further analysis. At a TE of 10 ms, the metabolite ratios are minimally affected by transverse relaxation values (for a typical T2 of 130 ms, this is 8%) but are affected by T1 and should largely be compared between control and experimental groups. Figure 1 shows example spectra from a control and 3-hour SE animal. In the MR spectroscopy data, a total of $n=28$ animals were studied (nine, each 1.5 hours and 3 hours) and $n=10$ controls. Quantitative T2 relaxometry was performed with Hahn spin echo imaging using 8 echo times with region of interest assignment as shown (Figure 2) in a separate set of animals. Least-square analysis based on a single exponential decay were performed using Bruker XTip software (Bruker Biospin, Billerica, MA, USA).

Statistical analyses were performed using two-tailed *t*-tests at $P<0.05$ for significance. Because of the anticipated variability in extent of injury between the hippocampi at this relatively early time frame of post-SE, i.e., local entry of kainate into the left and right hippocampus is independent of each other, all voxels were evaluated individually. To adequately assess R values of ~ 0.6 with power of 0.8 and significance of 0.05, $n=18$ samples were used in each group, i.e., $n=9$ rats. However, to more completely show the regression data in Table 1, we include all R values >0.4 together with their significance values. Regression and 95% confidence intervals on the line of means were calculated using MATLAB 2011b (The MathWorks, Natick MA, USA) and Microsoft Excel. Experimental outcomes were the continuous measurements in the spectroscopic, imaging, and histologic results.

RESULTS

Group Results

The 1.5- and 3-hour model animals differed slightly in terms of total kainate dosing, with the 1.5-hour group using a mean kainate dose of 19.4 ± 2.7 mg/kg and the 3-hours group 23.1 ± 4.2 mg/kg. This 19% difference was of borderline significance ($P=0.055$) between the two groups. Figures 1A and 1G show a scout, typical spectra and two examples of the fitted metabolites. Figure 1H shows the group results for the two SE groups and controls. There are significant changes in NAA/tCr, Ins/tCr, Gln/tCr, and lactate/tCr in both of the SE groups relative to control. These data verify the report of Filibian 2012,[5] finding neuronal dysfunction assessed through the NAA/tCr decline and glial activation from the increase in Ins/tCr.

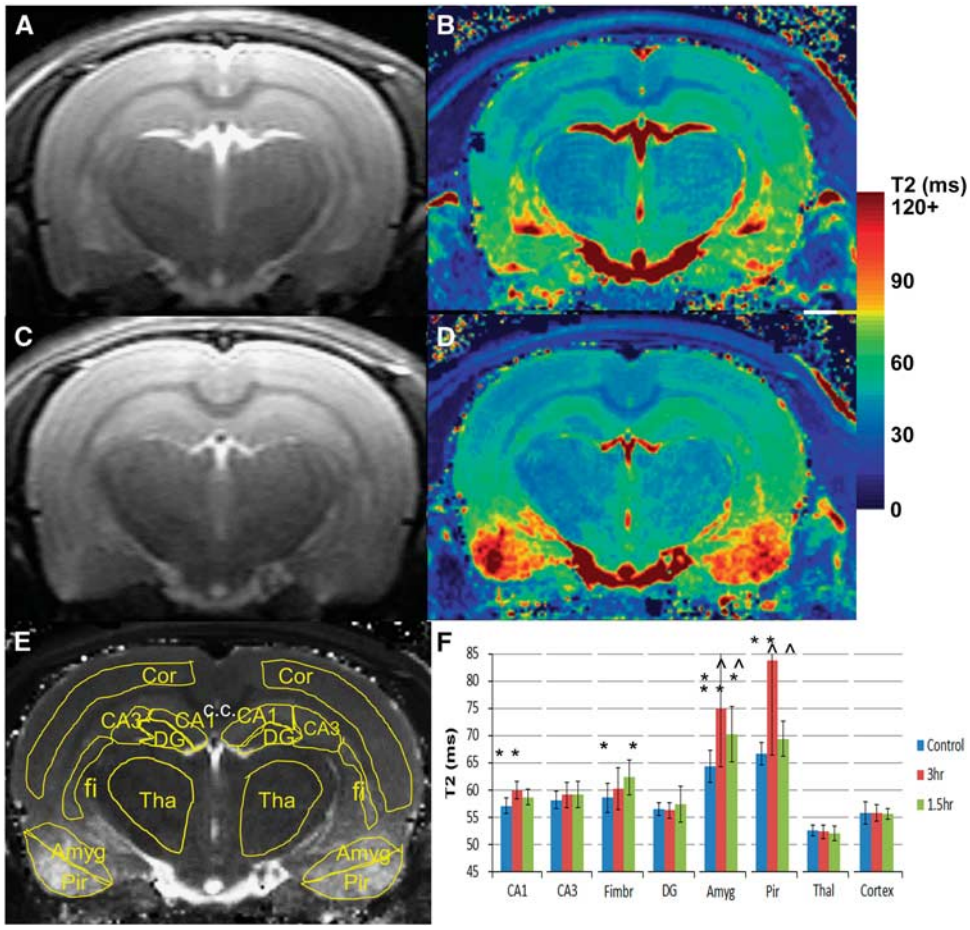

Figure 2. T2 relaxometry data from a control (**A** and **B**) and a 3-hour kainate rat (**C** and **D**), each showing the scout and T2 maps. The regions of interest used in the reported T2 values are shown in **E**. (**F**) Shows a column plot from all the data (means and s.d.). Amyg, amygdala; CA1, CA3; Cor neocortex; DG dentate gyrus; fi, fimbria; Pir, piriform cortex; Thal, thalamus. In **F**, symbol * indicates $P < 0.05$ comparing control with the 1.5- and 3-hour groups; symbol ^ indicates $P < 0.05$ significance comparing 1.5- and 3-hour groups.

Table 1. Pearson's correlation values between metabolites, 1.5- and 3-hour groups

	NAA/tCr	*Glu/tCr*	*GABA/tCr*	*Gln/tCr*	*GSH/tCr*
1.5 Hours					
Glu/tCr	+0.51; $P < 0.05$; Figure 4A				
GABA/tCr	+0.64; $P < 0.01$; Figure 4B	+0.48; $P < 0.05$			
Gln/tCr	n.s.	+0.53; $P < 0.05$; Figure 4D	+0.50; $P < 0.05$		
GSH/tCr	n.s.	n.s.	n.s.	n.s.	
Ins/tCr	n.s.	n.s.	n.s.	n.s.	n.s.
3 Hours					
Glu/tCr	+0.86; $P < 0.001$ Figure 4A				
GABA/tCr	+0.51; $P < 0.05$; Figure 4B	+0.42; $P = 0.10$			
Gln/tCr	n.s.	+0.45; $P = 0.08$; Figure 4D	n.s.		
GSH/tCr	n.s.	−0.62; $P < 0.03$	n.s.	−0.66; $P < 0.01$; Figure 4E	
Ins/tCr	n.s.	n.s.	n.s.	n.s.	n.s.

Gln, glutamine; Glu, glutamate; GSH, glutathione; Ins, myo-inositol; NAA, *N*-acetylaspartate; n.s., nonsignificant; tCr, total creatine. The *R* value is shown if >0.40 with its *P*-value. As the table is symmetric, only half the boxes are filled for each group. For several of the entries, the figure plot that shows the regression is indicated.

T2 relaxometry data are shown in Figure 2, including definition of the regions of interest. Showing the consistency of the measurement and the relatively well-controlled SE of the model (thus not inducing whole brain damage), there was no change in the T2 of cortex (55.8 ± 1.0 ms, $n = 5$ rats, control versus 55.4 ± 0.7 ms from the combined status groups $n = 5$, 3 hours; $n = 6$, 1.5 hours). Consistent with Roch *et al*,[4] significant increases in T2 were seen between the 1.5 hours and control in the fimbria, amygdala, and piriform cortex; in the 3-hour group these were in the CA1, amygdala, and piriform cortex. The 1.5- and 3-hour groups differed in the fimbria, amygdala, and piriform regions. Although the 3-hour group had the highest T2 values in the amygdala and piriform regions, the 3-hour group

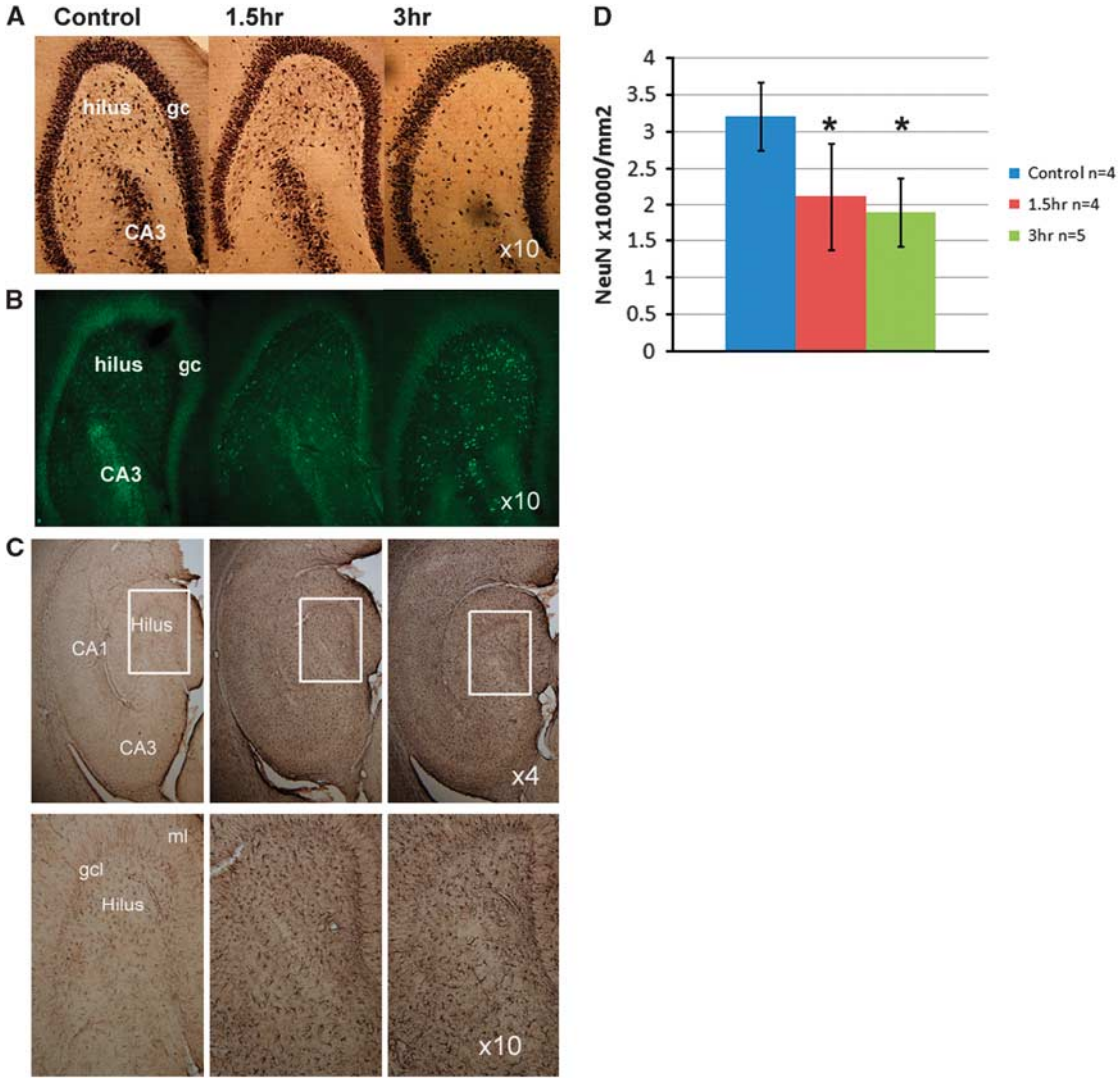

Figure 3. NeuN (**A**), Fluoro-Jade (**B**), and glial fibrillary acidic protein (GFAP; **C**) stained hippocampi from control, 1.5-, and 3-hour rats (shown in columns). In **C**, the top row shows the hippocampus at ×4 magnification with the identified inset boxes at ×10. (**D**) Shows tabulated NeuN counts from the hilus. For the NeuN counts, all kainate acid (KA) treated rats are significantly different from control, *$P < 0.05$. For histology, all animals were killed immediately after the imaging study, 3 days after the status epilepticus period.

fimbria T2 was not significantly different from control but was significantly shorter than the 1.5-hour group. There were no significant differences in either group from the CA3 region.

In all of the SE rats, Fluoro-Jade B staining revealed the presence of fluorescent degenerating neurons throughout the hippocampus. Variation in the staining density of neurons was apparent in the hilar region with the 1.5-hour SE rats showing a moderately lesser extent of degenerating neurons than the 3-hour rats. Glial fibrillary acidic protein staining was markedly elevated in both the 1.5- and 3-hour groups compared with control (Figure 3C) consistent with astrocytic activation. Quantification of neuron numbers in the hilus for NeuN-stained sections revealed that the SE rats had significantly fewer neurons than in the control group ($P < 0.001$, Figure 3), with a 40% to 50% loss in neurons in the 3-hour group.

Regression Analyses

Given that the SE is anticipated to induce a correlated set of metabolic changes, a Pearson's correlation table was generated for both status groups (Table 1). There was no significant correlation between kainate dose with any of the metabolites. In discussing these correlations, we consider the individual metabolites grouped in terms of their roles in neuronal injury, glial reaction, etc. None of these metabolites were correlated in the control group.

For the evaluation of neuronal function, we assessed how Glu/tCr, GABA/tCr, and NAA/tCr were correlated. For Glu/tCr and NAA/tCr, the 3-hour group was highly correlated at $R = +0.86$, $P < 0.001$ (Figure 4A), while the 1.5-hour group was correlated at $R = +0.51$, $P < 0.05$. For NAA/tCr and GABA/tCr, the 1.5-hour group showed a correlation of $R = +0.64$, $P < 0.01$; the 3-hour group was $R = +0.51$, $P < 0.05$ (Figure 4B). Given these correlations, it is not surprising that Glu/tCr and GABA/tCr are similarly linked. The relationships between NAA, Glu, and GABA are consistent with NAA characterizing both glutamatergic and GABAergic mitochondrial function.

The group increase in Ins/tCr is consistent with the literature and astrocytic activation occurring with SE.[5,26] This increase correlates with the quantitative T2 from the CA3 region for both the 1.5- and 3-hour groups, nearly identical at $R = -0.68$, $P < 0.025$, 1.5-hours group; $R = -0.64$ $P < 0.05$, 3-hour group (Figure 4C). This negative relationship supports the view that the animals with higher Ins/tCr maintained the shorter water relaxation values. Glial activation is also seen with the increased Gln/tCr, most likely

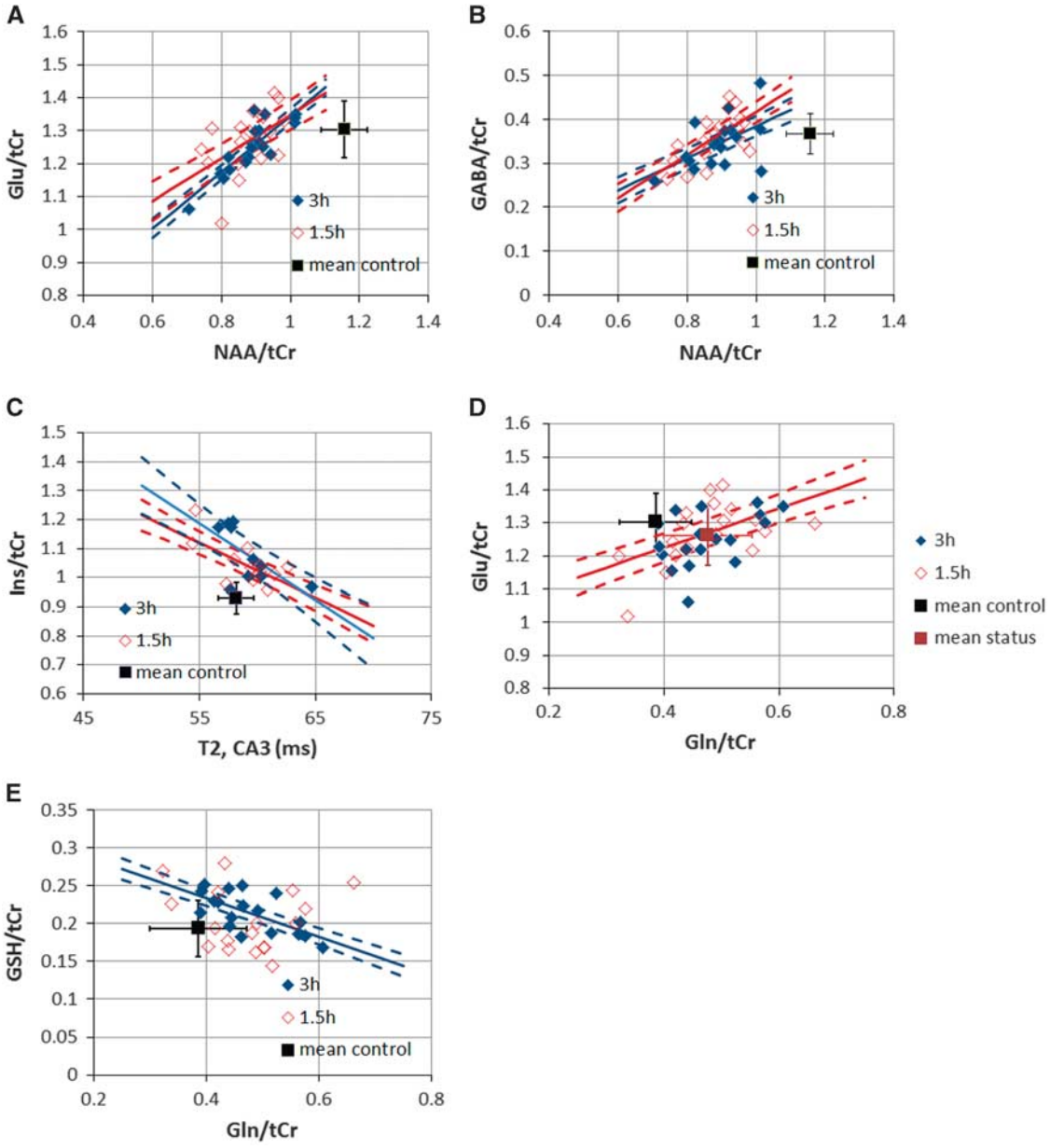

Figure 4. Scatterplots of metabolite parameters with control data are shown. For all plots, the indicated regression line (solid) and 95% confidence intervals (dashed) for the means are shown if significant. Data plotted in red are from 1.5 hours (also, open symbols), plotted in blue are 3-hour data (also, filled symbols). Control data mean and s.d. are plotted; none of the control data showed any significant regression values. (**A**) Glutamate/total creatine (Glu/tCr) with *N*-acetylaspartate (NAA)/tCr 3-hour group, $R = +0.86$, $P < 0.001$; 1.5-hour group, $R = +0.51$, $P < 0.05$. (**B**) GABA/tCr with NAA/tCr 3-hour group, $R = +0.51$, $P < 0.05$; 1.5-hour group, +0.64, $P < 0.005$. (**C**) CA3 T2 with myo-inositol/tCr (Ins/tCr) 3-hour group, $R = -0.63$, $P < 0.005$; 1.5-hour group, $R = -0.68$, $P < 0.02$. (**D**) Glutamine/tCr (Gln/tCr) with Glu/tCr 3-hour group, $R = +0.45$, nonsignificant with $P = 0.08$; 1.5-hour group, $R = +0.53$, $P < 0.05$. The combined mean and s.d. of the 1.5- and 3-hour groups for Glu/tCr and Gln/tCr are also shown (see text). (**E**) Gln/tCr with Glutathione/tCr (GSH/tCr) 3-hour group, $R = -0.66$, $P < 0.01$; 1.5-hour group nonsignificant. GABA, gamma-aminobutyric acid.

induced by the seizure activity and consequent neurotransmitter cycling. The increased Gln/tCr correlated with glutamatergic function Glu/tCr with $R = +0.53$, $P < 0.05$ in the 1.5-hour group (Figure 4D). In the 3-hour group, this relationship between Gln and Glu showed a trend for a linear relationship, with $R = +0.45$, $P = 0.08$.

As has been observed by Filibian 2012,[5] GSH is increased in the poststatus period, consistent with its decreased consumption with progressive neuronal injury. The present data finds a significant correlation in the 3-hour group between GSH/tCr with Gln/tCr ($R = -0.66$, $P < 0.01$; Figure 4E) and Glu/tCr ($R = -0.62$, $P < 0.025$ regression not shown), while it is not present in the shorter status group. Given this negative relationship where the lowest GSH/tCr occurs when Gln/tCr is high, this suggests that in conditions of high Gln or astrocytic activation, GSH is consumed at a higher rate.

DISCUSSION

Injury in the 1.5- and 3-hour Status Groups

These spectroscopic data confirm that whether with 1.5- or 3-hour SE, at the 3-day post-SE time point there is a decline in NAA/tCr

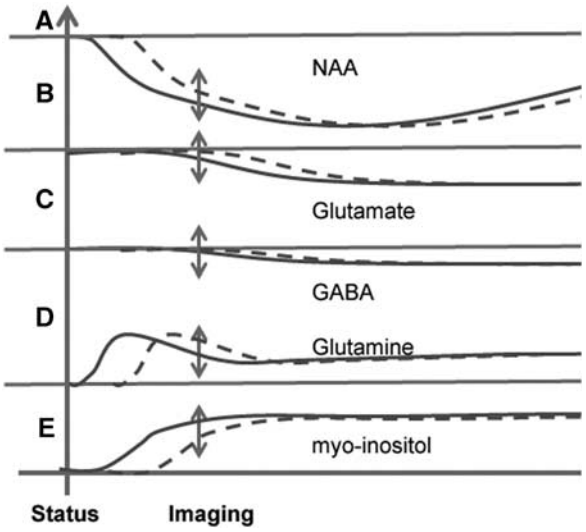

Figure 5. Hypothetical time courses of metabolic changes for (**A**) *N*-acetylaspartate/total creatine (NAA/tCr), (**B**) glutamate/tCr (Glu/tCr), (**C**) GABA/tCr, (**D**) glutamine/tCr (Gln/tCr), and (**E**) myo-inositol/tCr in the status/poststatus time period. Amplitudes are not drawn to scale. Control levels are indicated by the thick horizontal solid lines. Dashed line indicates an animal with a 'delayed onset' of injury and solid line an animal with an 'early onset' of injury. The double-headed arrows indicate the observed data spread at the time of the imaging study. The spread on NAA/tCr and Glu/tCr is such that the early-onset injured rat will have lower values for both NAA/tCr and Glu/tCr than the delayed-onset injured rat. In comparison, the spread on Glu/tCr and Gln/tCr is such that the early-onset rat will have higher Gln/tCr while Glu/tCr is lower; the delayed-onset rat will have lower Gln/tCr while Glu/tCr is higher.

consistent with the neuronal mitochondrial injury. This decline occurs at the same time that histologic data shows NeuN determined neuronal loss in the hilus and widespread Fluoro-Jade staining indicative of injured and degenerating neurons throughout the hippocampus. With glutamatergic neuronal function described by Glu/tCr, Figure 4A shows a 10% decrease in mitochondrial NAA/tCr before Glu/tCr and glutamatergic injury is manifest. Given the known slow turnover of NAA,[28] this 10% decrease is likely to represent an acute loss of neuronal mitochondrial function, with the further relationship of NAA/tCr with declining Glu/tCr (reaching a total mean decrease in NAA/tCr of ~25%) likely characterizing progressive glutamatergic dysfunction. A similar behavior is seen with NAA/tCr and GABA/tCr (Figure 4B). The high significance of the NAA–Glu relationship is consistent with the *in vivo* human reports finding that NAA and Glu are correlated in healthy and surgical epilepsy patients.[29,30]

Also seen in both status groups are significant relationships with Ins/tCr and quantitative T2 measurements from the CA3 region (Figure 4C). As shown by cellular and human studies,[16,30] Ins is believed to be in high concentration in astrocytes with its molecular role identified with the maintenance of cellular osmolality relative to extracellular fluid. This homeostatic response would thus be anticipated to be developed during and after SE, consistent with studies showing shifts in tissue osmolality[31] and glial activation.[26] T2 values are known to be dynamic in the poststatus period, changing temporally and regionally. In the hyperacute time frame (either during the seizure or at most a few hours after seizures), the T2 decreases,[20,32] consistent with increased deoxyhemoglobin content and increased cellular osmolarity (with decreased extracellular space) as suggested by Heinemann.[31] In the longer time frame, the T2 increases and then subsequently normalizes. As reported by Roch *et al*[4] and consistent with the present 3-day data, the amygdala and piriform cortex show substantial T2 increases, although it is unchanged in the CA3 region. In the CA3, the lack of T2 change may also relate to the volumetric maintenance of astrocytic cell bodies and processes in the transition from normal to reactive astrocytosis.[33] Nonetheless, as mentioned,[18,19] T2 values are strongly linked with a variety of factors that induce edema, neuronal injury, and osmolarity changes, with decreased T2 occurring with increased osmolarity. With Ins's role in maintenance of cellular osmolarity, the identified (negative) relationship between inositol and CA3 T2 is consistent with the efficacy of this homeostatic process at the 3-day time point. It is possible that the increased Ins may be a contributing factor to the limited changes in T2 seen in the fimbria, where the 3-hour group shows a shorter T2 than the 1.5-hour group.

As stated in the Introduction section, the present data are effectively cross-sectional in nature. Specifically, given the known variation in bioavailability of the kainate at a fixed dose, we anticipate that the varying temporal onset of injury will contribute to the observed spread in the group data. As diagrammed in Figures 5A and 5B, the spread of the NAA/tCr, Glu/tCr values can be because of 'early onset' (solid line) and 'delayed onset' (dashed line) injury. Regression analysis of these metabolic parameters would, depending on noise and dynamic range of values, exhibit the statistically significant positive correlations as experimentally observed. The observation that the neuronal parameters of NAA/tCr, Glu/tCr, and GABA/tCr give similar regressions from the 1.5- and 3-hour status groups suggests that the poststatus 3-day time courses of these parameters are similar between the two groups, consistent with the view that (not surprisingly) status-induced neuronal injury has been produced in both groups.

Glial Activation

The increased Gln/tCr in the 3- and 1.5-hour groups is consistent with the view of increased Glu clearance driven by seizure activity, this view also supported by Western blot results from Hammer *et al*[34] and more recently by Sun *et al*[35] who found increased Gln synthetase (GS) in the early phases of the epileptogenesis (kainate and amygdalar kindling models). The present data also show that the 1.5-hour group has a positive correlation $R = +0.53$, $P < 0.05$ between Gln/tCr and Glu/tCr, arguing that the increased Gln occurs under conditions of more intact glutamatergic function. However, if we hypothesize this situation to have evolved from the control condition, the observation of this positive correlation is of interest. Figure 4D shows the mean values of the combined status groups and for control. If the control group value serves as a starting point of consideration for the status groups, the simplest hypothesis that relates the status groups to the control data would project a relationship between the mean control value and the mean status value, which would produce either no regression or a negative regression. However, the observed positive correlation argues against this simple hypothesis.

One explanation for these observations may be a dynamic response of Gln. Although the above reports of Hammer and Sun have both identified an increase in GS activity in the latent period, several groups have found GS activity declines as astrocytes develop a reactive profile with progression from the acute into the chronic phase.[3,34,36] This would also be consistent with the present data, in which the initial increase in Gln/tCr occurring in response to seizure linked Glu neurotransmission is followed by a decrease in Gln/tCr toward apparent normalization. With the cross-sectional nature of the group data and variation in temporal onset of seizure with subsequent neuronal injury and glial dynamics (diagrammed in Figure 5D), a rise and then fall in Gln/tCr would generate the observed positive regression in relation to Glu/tCr. This positive regression could also be partly understood based on the recognition that decreased glutamatergic function, with its decrease in neurotransmission would result in decreased

Gln; however, this view does not provide good explanation for the increased Gln/tCr. Thus these data are consistent with an early increase in GS flux and content, with a decline in GS flux that follows as reactive astrocytosis develops.[3,34–36]

Short Versus Long Status Duration

As implicitly hypothesized in this study, with its greater sustained seizure period and near 100% rate in generating chronic epilepsy, the metabolic changes and processes seen in the 3-hour group may not necessarily match that of the 1.5-hour group. The present data are consistent with this, finding significant correlations with GSH/tCr in the 3-hour but not the 1.5-hour group. In the 3-hour group, GSH/tCr correlates with both Gln/tCr at $R = -0.66$, $P < 0.01$ (Figure 4E) and Glu/tCr ($R = -0.62$, $P < 0.025$ regression not shown). As a negative regression, animals with higher Gln/tCr has a normal to low GSH/tCr (right side of Figure 4E), consistent with glial activation, relatively normal glutamatergic function and continuing consumption of GSH. On the left side of Figure 4E, the lower Gln/tCr has the higher GSH/tCr, consistent with progressive glutamatergic dysfunction, decreased GS function and decreased GSH consumption. With GSH interacting in both astrocytic (where it is synthesized) and neuronal compartments (for review see Dringen *et al*[37]), this is consistent with its function with neuronal antioxidant consumption, as well as with the report from Filibian *et al*.[5]

The 1.5-hour group does not show a clear relationship between GSH/tCr and Gln/tCr. The basis for this difference may be complex, possibly as a mix of multiple processes with differing time courses (e.g., GSH rapidly being consumed in the neuronal pool while there is also increased glial synthesis). Another explanation for this could be volume extent of injury in the CA3 region studied, e.g., with the 1.5-hour group exhibiting partial injury, while the 3-hour group has achieved the larger extent of metabolic injury. It should be noted, however, from the NAA/tCr, Glu/tCr dynamic ranges seen in Figure 4A that there is nearly complete overlap in these parameters between the 3- and 1.5-hour groups and thus a hypothetical volumetric injury difference is unlikely to be the only cause for the GSH/tCr regression differences. The GSH regressions in the long status group is thus likely representing a process of maturation of injury, consistent with the apparently slower increase in GSH/tCr as reported by Filibian *et al*.[5]

Caveats

The major caveats in this work rest on three issues, the use of metabolite ratios to total creatine rather than absolute concentrations, the qualitative difficulty of assessing seizure severity during the status period, and the termination of seizures. First, as stated in the Introduction section, the metabolite ratios in this study are considered as functional measures rather than strict concentrations. This is based on the view that the ratios can be more informative than concentrations alone because of the interest in understanding concentrations in terms of functioning mass, taken here as the size of the tissue's creatine kinase buffering system and measured by total creatine.[15,38] Quantification measures based on tissue water or other reference would not provide this normalization. However, it is nonetheless important to consider how stable the total creatine pool is. Reports on the stability of the total creatine tCr pool in such models are few; Gupta *et al*[39] studied acetylcholinesterase models of seizures and found no significant change in tCr at 3 days in the hippocampus and amygdala although at 1 hour after seizures there is a 25% decline. Clearly, changes in creatine metabolism can affect the observations; for example, if there is a decrease in total creatine as suggested from the 1-hour time point of Gupta *et al*,[39] the interpretation of the decline in NAA/tCr and Glu/tCr would mean that mitochondrial and glutamatergic function is more compromised than expected when compared with functioning cellular mass, while the increase in Ins/tCr would mean potentially less glial reaction. Given the well-described glial activation occurring in this model in the literature, we nonetheless think that changes in total creatine in this time frame will not be so large as to eliminate the observations for increased glial activation as assessed with inositol and Gln.

Second, while the Racine classification[21] is robust for identifying behavioral seizures, the identification of less intense seizures is variable. Our assessments of kainate dosing, seizure count, and metabolites showed no sensitivity, consistent with other descriptions of this model.[9] Finally, the use of diazepam to terminate the seizures can be problematic as it has been reported that abnormal EEG activity can persist although behavioral events resolve. Whether this difference is pertinent has been debated (e.g., there is no difference in latency to recurrent seizure onset between animals that required extra diazepam versus those that did not[40]) but the greatest effect this will have on the present data would be to result in variability and a longer seizure period especially with the 3-hour group. However, as our interest lies in variability in these two groups, this is unlikely to be a problem for the metabolic and T2 effects reported here.

CONCLUSIONS

In the post-SE time frame, we believe that understanding the distortion of metabolism is pertinent to better target cellular compartments (glial versus neuronal) for potential therapeutic effect and to potentially provide biomarkers for epileptogenesis (rather than solely neuronal injury). Thus in this report, the Hellier–Dudek kainate model of epilepsy has been studied with MR spectroscopy, T2 imaging and histologic analysis using two durations of SE, 1.5 and 3 hours. As expected, the neuronal injury evaluated by NAA/tCr, Glu/tCr, and GABA/tCr was significantly correlated in both groups. Also in both groups, quantitative T2 values in the CA3 region was significantly correlated with Ins/tCr, consistent with the known role of Ins in responding to osmotic shifts and glial activation. More clearly identified in the 1.5-hour group compared with the 3-hour group, there was a significant positive relationship between Gln/tCr with Glu/tCr. It is noted that this positive relationship is likely to arise from an initial Gln/tCr increase in response to neurotransmission cycling and increased GS activity, with a subsequent decline as the glutamatergic injury develops. Significant relationships between GSH/tCr, Gln/tCr, and Glu/tCr are seen in the 3-hour group but not in the 1.5-hour group, consistent with the notion that as the SE injury matures, Gln decreases toward a pseudonormalized level, which in the context of glutamatergic injury, is accompanied by higher GSH/tCr. Whether these metabolic and imaging changes relate to the subsequent development of recurrent seizures will require more work; however, the metabolic response during and after status clearly evolves with a time course that relates to status duration and reflects neuronal injury interacting with early and later glial activation, accompanied by slower changes in GSH as neuronal injury progresses.

AUTHOR CONTRIBUTIONS

YW acquired the imaging data and participated in the analysis and interpretation. PSP created the epilepsy model, prepared the animals for imaging, and participated in the interpretation. AR performed the histologic analysis. TKH assisted in the setup of the imaging experiments. NCdL assisted in the interpretation and oversight of the histologic analysis. JWP participated in the imaging and model setup, analysis, and data interpretation.

DISCLOSURE/CONFLICT OF INTEREST

The authors declare no conflict of interest.

REFERENCES

1 Kudin AP, Zsurka G, Elger CE, Kunz WS. Mitochondrial involvement in temporal lobe epilepsy. *Exp Neurol* 2009; **218**: 326–332.
2 Waldbaum S, Patel M. Mitochondrial dysfunction and oxidative stress: a contributing link to acquired epilepsy? *J Bioenerg Biomembr* 2010; **42**: 449–455.
3 Eid T, Thomas MJ, Spencer DD, Rundén-Pran E, Lai JC, Malthankar GV *et al.* Loss of glutamine synthetase in the human epileptogenic hippocampus: possible mechanism for raised extracellular glutamate in mesial temporal lobe epilepsy. *Lancet* 2004; **363**: 28–37.
4 Roch C, Leroy C, Nehlig A, Namer IJ. Predictive value of cortical injury for the development of temporal lobe epilepsy in 21-day-old rats: an MRI approach using the lithium-pilocarpine model. *Epilepsia* 2002; **43**: 1129–1136.
5 Filibian M, Frasca A, Maggioni D, Micotti E, Vezzani A, Ravizza T. In vivo imaging of glia activation using 1H MRS to detect putative biomarkers of tissue epileptogenicity. *Epilepsia* 2012; **53**: 1907–1916.
6 Berg AT, Shinnar S. Unprovoked seizures in children with febrile seizures: short term outcome. *Neurology* 1996; **47**: 562–568.
7 Hellier JL, Dudek FE. Chemoconvulsant model of chronic spontaneous seizures. *Curr Protoc Neurosci* 2005; **9**: 9–19.
8 Williams PA, White AM, Clark S, Ferraro DJ, Swiercz W, Staley KJ *et al.* Development of spontaneous recurrent seizures after kainate-induced status epilepticus. *J Neurosci* 2009; **29**: 2103–2211.
9 Lévesque M, Avoli M. The kainic acid model of temporal lobe epilepsy. *Neurosci Biobehav Rev* 2013; **37**(10 Pt 2): 2887–2899.
10 Kondratyev A, Gale K. Latency to onset of status epilepticus determines molecular mechanisms of seizure-induced cell death. *Brain Res Mol Brain Res* 2004; **121**: 86–94.
11 Bates T, Strangward M, Keelan J, Davey G, Munro P, Clark J. Inhibition of NAA production: implications for 1H MRS studies in vivo. *Neuroreport* 1996; **7**: 1397–1400.
12 Pan JW, Takahashi K. Inter-dependence of NAA and high energy phosphates in human brain. *Ann Neurol* 2005; **57**: 92–97.
13 Vielhaber S, Niessen HG, Debska-Vielhaber G, Kudin AP, Wellmer J, Kaufmann J *et al.* Subfield-specific loss of hippocampal N-acetyl aspartate in temporal lobe epilepsy. *Epilepsia* 2008; **49**: 40–50.
14 Tkác I, Rao R, Georgieff MK, Gruetter R. Developmental and regional changes in the neurochemical profile of the rat brain determined by in vivo 1H NMR spectroscopy. *Magn Reson Med* 2003; **50**: 24–32.
15 Connett RJ. Analysis of metabolic control: new insights using scaled creatine kinase model. *Am J Physiol* 1988; **254**(6 Pt 2): R949–R959.
16 Strange K, Emma F, Paredes A, Morrison R. Osmoregulatory changes in myo-inositol content and Na+/myo-inositol cotransport in rat cortical astrocytes. *Glia* 1994; **12**: 35–43.
17 Schneider S. Inositol transport proteins. *FEBS Lett* 2015; **589**: 1049–1058.
18 Jolesz FA. Compartmental analysis of brain edema using magnetic resonance imaging. *Acta Neurochir Suppl (Wien)* 1994; **60**: 179–183.
19 Vajda Z, Berényi E, Bogner P, Repa I, Dóczi T, Sulyok E. Brain adaptation to water loading in rabbits as assessed by NMR relaxometry. *Pediatr Res* 1999; **46**: 450–454.
20 Choy M, Dubé CM, Patterson K, Barnes SR, Maras P, Blood AB *et al.* A novel, noninvasive, predictive epilepsy biomarker with clinical potential. *J Neurosci* 2014; **34**: 8672–8684.
21 Racine RJ. Modification of seizure activity by electrical stimulation. II. Motor seizure. *Electroencephalogr Clin Neurophysiol* 1972; **32**: 281–294.
22 Schmued LC, Hopkins KJ. Fluoro-Jade B: a high affinity fluorescent marker for the localization of neuronal degeneration. *Brain Res* 2000; **874**: 123–130.
23 Shu SY, Ju G, Fan LZ. The glucose oxidase-DAB-nickel method in peroxidase histochemistry of the nervous system. *Neurosci Lett* 1988; **85**: 169–171.
24 Miyasaka N, Takahashi K, Hetherington HP. 1H NMR spectroscopic imaging of the mouse brain at 9.4 T. *J Magn Reson Imaging* 2006; **24**: 908–913.
25 Provencher SW. Estimation of metabolite concentrations from localized in vivo proton NMR spectra. *Magn Reson Med* 1993; **30**: 672–679.
26 Torre ER, Lothman E, Steward O. Glial response to neuronal activity: GFAP-mRNA and protein levels are transiently increased in the hippocampus after seizures. *Brain Res* 1993; **631**: 256–264.
27 Choi IY, Gruetter R. Dynamic or inert metabolism? Turnover of N-acetyl aspartate and glutathione from D-[1-13C]glucose in the rat brain in vivo. *J Neurochem* 2004; **91**: 778–787.
28 Pan JW, Venkatraman T, Vives K, Spencer DD. Quantitative glutamate spectroscopic imaging of the human hippocampus. *NMR Biomed* 2006; **19**: 209–216.
29 Degnan A, Ceschin R, Lee V, Schmithorst V, Bluml S, Panigrahy A. Early metabolic development of posteromedial cortex and thalamis in humans analyzed via an in vivo quantitative MR spectroscopy. *J Comp Neurol* 2014; **522**: 3717–3732.
30 Videen JS, Michaelis T, Pinto P, Ross BD. Human cerebral osmolytes during chronic hyponatremia. A proton magnetic resonance spectroscopy study. *J Clin Invest* 1995; **95**: 788–793.
31 Heinemann U. Excitatory amino acids and epilepsy-induced changes in extracellular space size. *Adv Exp Med Biol* 1986; **203**: 449–460.
32 van Eijsden P, Notenboom RG, Wu O, de Graan PN, van Nieuwenhuizen O, Nicolay K *et al.* In vivo 1H magnetic resonance spectroscopy, T2-weighted and diffusion-weighted MRI during lithium-pilocarpine-induced status epilepticus in the rat. *Brain Res* 2004; **1030**: 11–18.
33 Wilhelmsson U, Bushong EA, Price DL, Smarr BL, Phung V, Terada M *et al.* Redefining the concept of reactive astrocytes as cells that remain within their unique domains upon reaction to injury. *Proc Natl Acad Sci USA* 2006; **103**: 17513–17518.
34 Hammer J, Alvestad S, Osen KK, Skare Ø, Sonnewald U, Ottersen OP. Expression of glutamine synthetase and glutamate dehydrogenase in the latent phase and chronic phase in the kainate model of temporal lobe epilepsy. *Glia* 2008; **56**: 856–868.
35 Sun HL, Zhang SH, Zhong K, Xu ZH, Feng B, Yu J *et al.* A transient upregulation of glutamine synthetase in the dentate gyrus is involved in epileptogenesis induced by amygdala kindling in the rat. *PLoS One* 2013; **8**: e66885.
36 Ortinski PI, Dong J, Mungenast A, Yue C, Takano H, Watson DJ *et al.* Selective induction of astrocytic gliosis generates deficits in neuronal inhibition. *Nat Neurosci* 2010; **13**: 584–591.
37 Dringen R, Gutterer JM, Hirrlinger J. Glutathione metabolism in brain metabolic interaction between astrocytes and neurons in the defense against reactive oxygen species. *Eur J Biochem* 2000; **267**: 4912–4916.
38 Ellington WR. Evolution and physiological roles of phosphagen systems. *Annu Rev Physiol* 2001; **63**: 289–325.
39 Gupta RC, Milatovic D, Dettbarn WD. Depletion of energy metabolites following acetylcholinesterase inhibitor-induced status epilepticus: protection by antioxidants. *Neurotoxicology* 2001; **22**: 271–282.
40 Drexel M, Preidt A, Sperk G. Sequel of spontaneous seizures after kainic acid-induced status epilepticus and associated neuropathological changes in the subiculum and entorhinal cortex. *Neuropharmacology* 2012; **63**: 806–817.